NEW FORMULATION OF THE SPACE–TIME FINITE ELEMENT METHOD FOR PROBLEMS OF EVOLUTION

Czesław Bajer Roman Bogacz

November 23, 1994

Polish Academy of Sciences,
Institute of Fundamental Technological Research,
Świętokrzyska 21, 00–049 Warszawa, Poland.

The work has been done as a part of the project
No PB–309389101, granted by KBN

1 Introduction

The space–time discretization of the structure has some advantages. First, it enables the non–stationary partition of a structure. It allows to solve in a simple way quite new problems: problems with moving edge, mesh adaptation in hyperbolic problems, mesh condensation which moves together with a travelling force. Second, the evolution of the domain considered in nonlinear problems can be efficiently modelled by the continuous change of geometry in time. The method of the space–time finite elements, described for the first time by Oden [1] and then developed in papers [2, 3, 4, 5] has considerably been changed as compared with its first formulation. The fundamental difference concerns the approximation of characteristic parameters. In commonly used time integration schemes it has the form

$$\boldsymbol{u}(\boldsymbol{x},t) = \boldsymbol{N}(\boldsymbol{x}) \cdot \boldsymbol{q}(t) \ , \tag{1}$$

whereas in the space–time approximation we use

$$\boldsymbol{u}(\boldsymbol{x},t) = \boldsymbol{N}(\boldsymbol{x},t) \cdot \boldsymbol{q}_e \ . \tag{2}$$

The same question concerns both the state parameters and the geometry of a structure. Thus the evolution of the geometry has a continuous representation in the formulation and in the equilibruim equation.

In the paper we will discuss some numerical properties of the time integration method derived from the formula (2). The first approach to the formulation developed here can be found in [6, 7]. The reader can also find there the historical background. It should be emphasized that we do not apply directly the Hamilton principle (nor any other energy methods). The method has various possibilities of modifications. The order of the error can be evaluated and changed according to our requirements. The artificial damping can easily be introduced and controlled. Engineering problems with the evolution of geometry can be solved with much more higher efficiency than with the use of other numerical tools. The approach can be extended to non–linear evolution of geometry within the time interval. It could allow

us to increase considerably the time step of calculation with material and geometrical nonlinearities. Thermo–mechanical coupling, temperature problems, problems with phase change can be modelled in a natural way by using non–rectangular space–time elements.

Let us shortly recall and develop the formulation.

2 Formulation

We start from the differential equation of motion

$$m\frac{dv}{dt} + kx = 0 \ . \tag{3}$$

The principle of virtual power gives the form

$$\left(m\frac{dv}{dt} + kx\right) v^* = 0 \ , \tag{4}$$

where v^* is the function of virtual velocity.

We assume the linear distribution of real velocity v over the time internal $0 \leq t \leq h$.

$$v = \left(1 - \frac{t}{h}\right) v_0 + \frac{t}{h} v_1 \ . \tag{5}$$

The displacement $x(t)$ is described by the integral

$$x(t) = \int_0^t v \, dt = h_0 + \frac{h}{2}\left[1 - \left(1 - \frac{t}{h}\right)^2\right] v_0 + \frac{t^2}{2h} v_1 \ . \tag{6}$$

Here the proper choice of distribution of the virtual velocity v^* is the fundamental problem of the method. The convergence, efficiency, accuracy of time integration and accuracy of the solution in the case of geometrical nonlinearities depend on the form of v^*. The simplest one is the Dirac distribution:

$$v^* = v_1 \, \delta\left(\frac{t}{h} - \alpha\right) \quad , \quad 0 \leq \alpha \leq 1 \tag{7}$$

The form (7) is convenient for our purpose since it reduces the computational effort and allows us to select the parameter α according to the stability condition.

The integration of (4) in time interval $[0, h]$, with respect to (5), (6) and (7) gives the following formula:

$$v_1 = \frac{1 - \frac{kh^2}{2m}[1 - (1-\alpha)^2]}{1 + \frac{k\alpha^2 h^2}{2m}} v_0 - \frac{k}{m} \frac{h}{\left(1 + \frac{k\alpha^2 h^2}{2m}\right)} x_0 \ , \tag{8}$$

which allows us to compute v_1 if the initial conditions v_0, x_0 for time step $[0, h]$ are known. Now the geometry x_1 is the last unknown value we must determine to proceed to the next step $[h, 2h]$. The average value of the velocity taken at point βh, $0 \leq \beta \leq 1$ results in the formula

$$x_1 = x_0 + h[(1-\beta)v_0 + \beta v_1] \ . \tag{9}$$

The energy at the end of the time interval is preserved if $\beta = 1 - \alpha$. Then we have finally

$$x_1 = x_0 + h[\alpha v_0 + (1-\alpha)v_1] \ . \tag{10}$$

It was proved in [7] that the unconditional stability of the process (8), (10) occurs for $\frac{\sqrt{2}}{2} \leq \alpha \leq 1$. For α=1 we have the explicit formula while for other values ($0 \leq \alpha < 1$) the scheme is implicit and requires iterations to determine the geometry x_1.

3 Numerical dissipation

Numerical damping of higher frequencies with zero damping of the basic frequency of the structure is the important question for each time integration method. Several papers on this subject exist (for example [8]). The ideal solution is when we can control the damping properties of the procedure (in particular cases the damping should be equal to zero). Lower frequencies should not be damped while higher should be damped relatively stronger. With respect to the shape of the damping diagram we can divide all methods in two groups: the first one (Wilson, Houbolt method) with the zero slope of the damping function for small h/T, growing with the increase of h/T, and the second one (Newmark, trapezoidal rule) with a certain slope of the damping function for $h/T \to 0$. The practical experiences indicate that

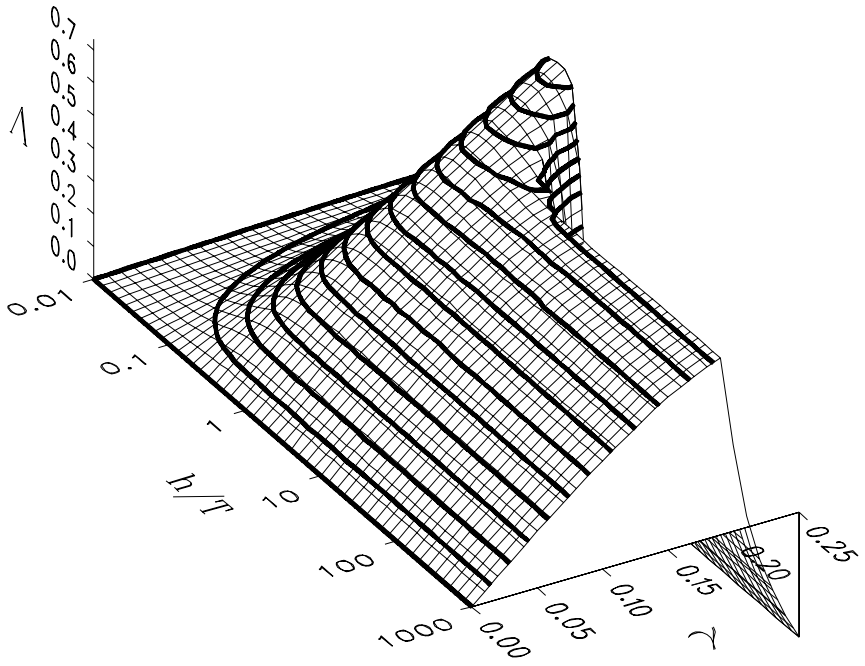

Figure 1: Logarithmic decrement Λ as a function of damping parameter γ for α=0.8.

the first group damps higher modes too much, and the second group does the same with lower modes. Other methods, which use more artificial parameters in their formulations, improve the damping properties but their use is dangerous since the regular dependence of properties on the parameters does not exist.

Here, let us modify the Eq. (9) by

$$\beta = 1 - \frac{\alpha}{1+\gamma} \quad , \quad 0 \leq \gamma \leq 1 \ . \tag{11}$$

The system (8), (9), (11) has the artificial damping which depends on the parameter γ and on the moment αh in which the equation of motion is considered. Figures 1 and 2 present the damping decrement as a function of γ for two values at α: 0.8 and 0.9. It can be interesting to compare the response of a 40–element model of a bar fixed at one end and subjected to an impulse. The most characteristic results are depicted in Fig. 3. Even small value of γ allows to reduce the spurious vibrations of higher modes. For the Courant number κ=1 ($\kappa = ch/b$, c – wave speed, b – length of the finite element) it suffices to take γ=0.05$\div$0.10. For short time steps γ should

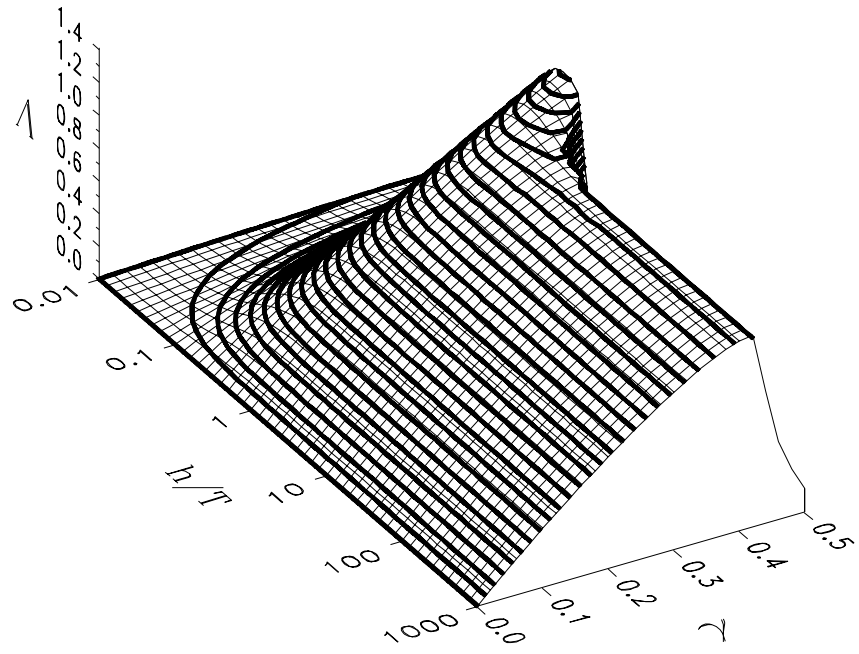

Figure 2: Logarithmic decrement Λ as a function of damping parameter γ for α=0.9.

Table 1: The order of convergence for different parameters α.

method	error order	coefficient
$\alpha = 0$	Δt^2	$\frac{1}{2}$
$\alpha = \frac{1}{4}$	Δt^2	$\frac{1}{4}$
$\alpha = \frac{1}{2}$	Δt^3	$\frac{1}{12}$
$\alpha = \frac{3}{4}$	Δt^2	$\frac{1}{4}$
$\alpha = 1$	Δt^2	$\frac{1}{2}$

be increased. Fig. 4 presents the displacement in time of the free end of the same bar. However, the calculation was performed with a long time step. Small artificial damping with γ=0.1 stabilizes vibration after several steps. Otherwise the response of the numerical model does not correspond with the response of the mathematical one.

4 Convergence

Simple error analysis enables us to determine the reminder of the Taylor expansion of the exact solution which is not represented in the numerical solution. The order of the error and respective coefficients for different parameters α are given in Table 1. The best case is for $\alpha = 1/2$. However, the scheme is conditionally stable. We can decrease the error order and improve the stability by a linear combination of several Dirac peaks introduced to (7). Then the virtual velocity has the form

$$v^* = v_1 \sum_i w_i \delta \left(\frac{t}{h} - \alpha_i \right) \ , \tag{12}$$

where w_i are the weights and α_i are the coordinates of peaks. The formula which corresponds to (8) is of the form

$$v_1 = \frac{1 - \frac{h^2}{2}[1 - \sum_i w_i (1 - \alpha_i)^2]}{1 + \frac{h^2}{2} \sum_i w_i \alpha_i^2} v_0 - \frac{h}{1 + \frac{h^2}{2} \sum_i w_i \alpha_i^2} x_0 \tag{13}$$

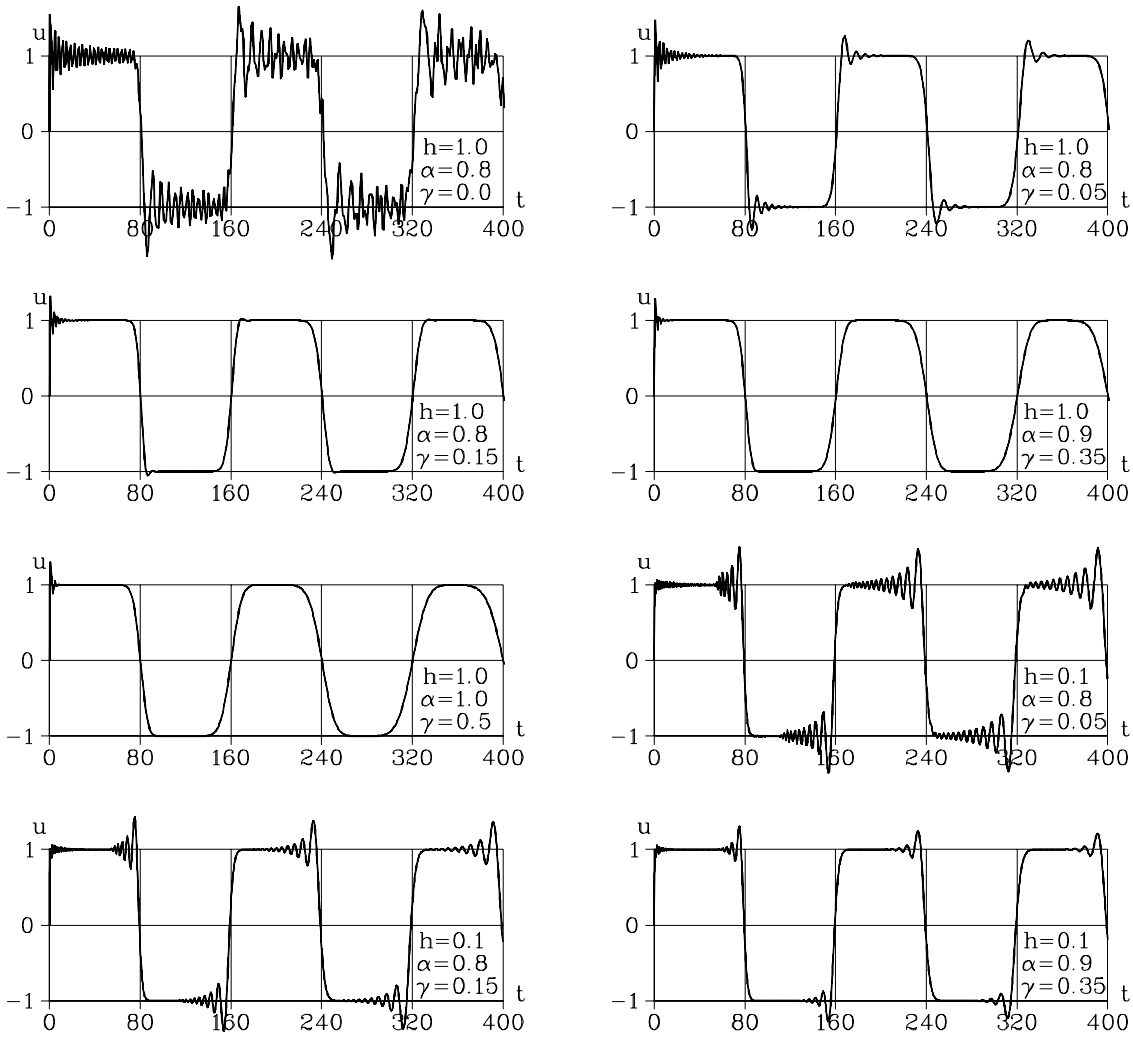

Figure 3: Displacements in time of the free end of the 40–element bar with selected parameters α and γ for time step h=0.1 and 1.0.

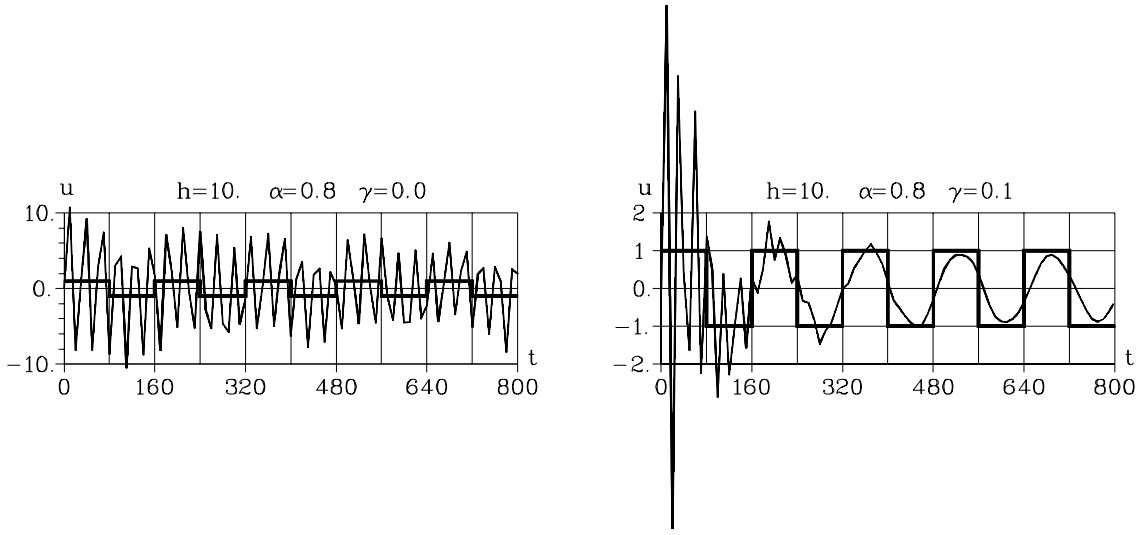

Figure 4: Displacements in time of the free end of a 40–element bar computed with a long time step: without damping and with γ=0.1 (thick line – theoretical solution).

Both k and m are, for simplicity, equal to 1. For example, if we take α_1=0, α_2=1/2, α_3=1, we can determine w_1=5/6, $w_2 = -2/3$, w_3=5/6. The solution has the error $O(h^4)$. The time integration scheme

$$v_1 = \frac{1 - \frac{h^2}{6}}{1 + \frac{h^2}{3}} v_0 - \frac{h}{1 + \frac{h^2}{3}} x_0 \ , \quad x_1 = x_0 + \frac{1}{2} h (v_0 + v_1) \tag{14}$$

is identical with the classical space–time finite element scheme described in [9]. We should strongly emphasize here that the coincidence occurs for the simplest case of a linear, one–degree–of–freedom system. Here we investigate such a case for the reason of its simplicity and possibility of comparison of the results. We can notice that in the case of linear vibration of simple oscillator, the central difference method is identical with the velocity formulation for $\alpha = 0$. The Newmark method ($\beta = \frac{1}{4}$, $\gamma = \frac{1}{2}$) and the trapezoid rule are identical with the case of $\alpha = \frac{\sqrt{2}}{2}$.

Higher ranges of approximation are also available. In the case described above by (14) the cost of calculations is doubled (in a general case of multi–degree-of–freedom system). Matrices have to be determined for $t = h/2$ and $t = h$. The matrix for $t = 0$ is taken from the previous step.

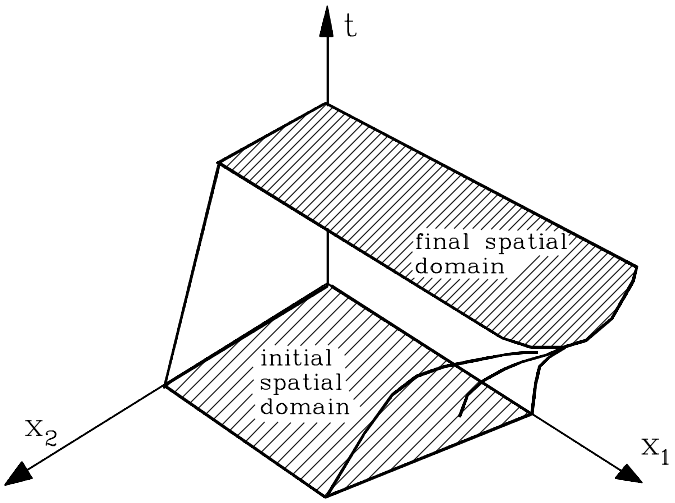

Figure 5: Evolution of the spatial domain in two dimensions.

The phase error P for the method described by (8), (10) is given by the relation

$$P = \frac{\sqrt{\kappa}}{\mathrm{arctg}\left(\frac{\sqrt{\kappa(2\alpha^2\kappa+4-\kappa)}}{\alpha^2\kappa+2-\kappa}\right)} \quad , \quad \kappa = \frac{ch}{b} \tag{15}$$

In the limit $\lim_{\kappa\to 0} P = 0$.

5 Multidimensional case

As a multidimensional case, let us consider the change of the geometry in time (Fig. 5). The equation of virtual work and the recurrence solution scheme is derived in the same way as in the case of one degree of freedom. The integration is carried out over the space time volume Ω:

$$\int_\Omega (\boldsymbol{v}^*)^T \rho \frac{\partial \boldsymbol{v}}{\partial t} \mathrm{d}\Omega + \int_\Omega (\dot{\boldsymbol{\varepsilon}}^*)^T \boldsymbol{\sigma} d\Omega = \int_\Omega (\boldsymbol{v}^*)^T \boldsymbol{f} \, \mathrm{d}\Omega \tag{16}$$

The displacement is described by the integral

$$\boldsymbol{u}(t) = \boldsymbol{u}_0 + \int_0^t \boldsymbol{v} \, \mathrm{d}t \quad . \tag{17}$$

The interpolation formulas

$$\boldsymbol{v} = \boldsymbol{N}\dot{\boldsymbol{q}} \quad \text{and} \quad \boldsymbol{v}^* = \boldsymbol{N}^*\dot{\boldsymbol{q}} \tag{18}$$

and constitutive equation $\boldsymbol{\sigma} = \boldsymbol{E}\boldsymbol{\varepsilon}$ allow us to write the equilibrium of forces in the time layer $[0, h]$ in the form

$$(\boldsymbol{K} + \boldsymbol{M})\dot{\boldsymbol{q}} = \boldsymbol{F} - \boldsymbol{s} \tag{19}$$

where

$$\boldsymbol{K} = \int\int_{V_{\alpha h}} (\mathcal{D}\boldsymbol{N}_{\alpha h}(\boldsymbol{x}))^T \boldsymbol{E}\mathcal{D}\boldsymbol{N}(\boldsymbol{x}, \frac{\alpha h}{2})\, \mathrm{d}V \cdot \alpha h \ , \tag{20}$$

$$\boldsymbol{M} = \int\int_{V_{\alpha h}} \boldsymbol{N}^T_{\alpha h}(\boldsymbol{x})\rho\frac{\partial \boldsymbol{N}(\boldsymbol{x}, \alpha h)}{\partial t})\, \mathrm{d}V \ , \tag{21}$$

$$\boldsymbol{s} = \int\int_{V_{\alpha h}} (\mathcal{D}\boldsymbol{N}_{\alpha h}(\boldsymbol{x})^T \boldsymbol{E}\boldsymbol{\varepsilon}_0\, \mathrm{d}V \ , \tag{22}$$

$$\boldsymbol{F} = \int\int_{V_{\alpha h}} \boldsymbol{N}^T_{\alpha h}(\boldsymbol{x}) \cdot \boldsymbol{f}(\boldsymbol{x}, \alpha h)\, \mathrm{d}V \ . \tag{23}$$

$\boldsymbol{K}$, $\boldsymbol{M}$, $\boldsymbol{s}$ and $\boldsymbol{F}$ are the stiffness matrix, mass matrix, initial internal force vector and external force vector, respectively. Here the integration is carried out over the spatial volume V. Shape matrices $\boldsymbol{N}_{\alpha h}$ are determined for the spatial geometry in $t = \alpha h$ and $\boldsymbol{N}(\boldsymbol{x}, \cdot)$ for the space–time volume in a given time.

Two numerical tests prove the efficiency of the method. The first one presents vibration of a bar element, fixed at one end. Very soft material ensures large displacements, comparing with the initial element length b=1.0. Two plots in Fig. 6 present the motion in the phase plane. They are obtained for the initial condition v_0=1.0. The first one was performed for h=0.1 and for different values of α. The second one compares the results for h=0.5 obtained by the space–time procedure (solid line) and by the modified Newton–Raphson method with central difference method for time integration (dashed line). The precision of the calculation is sufficiently high in spite of the large geometry change per step. The second test was performed for the viscoplastic material. The Norton constitutive law [10] was taken for calculation. The 3×3 finite element square hits a rigid base with the initial speed v_0. Displacement of the upper corner as a function of time is depicted in Fig. 7. Different time steps were taken. The fastest calculation was obtained for h=5 with α=0.5 (5 steps with 3–4 iterations per step). The second interesting case

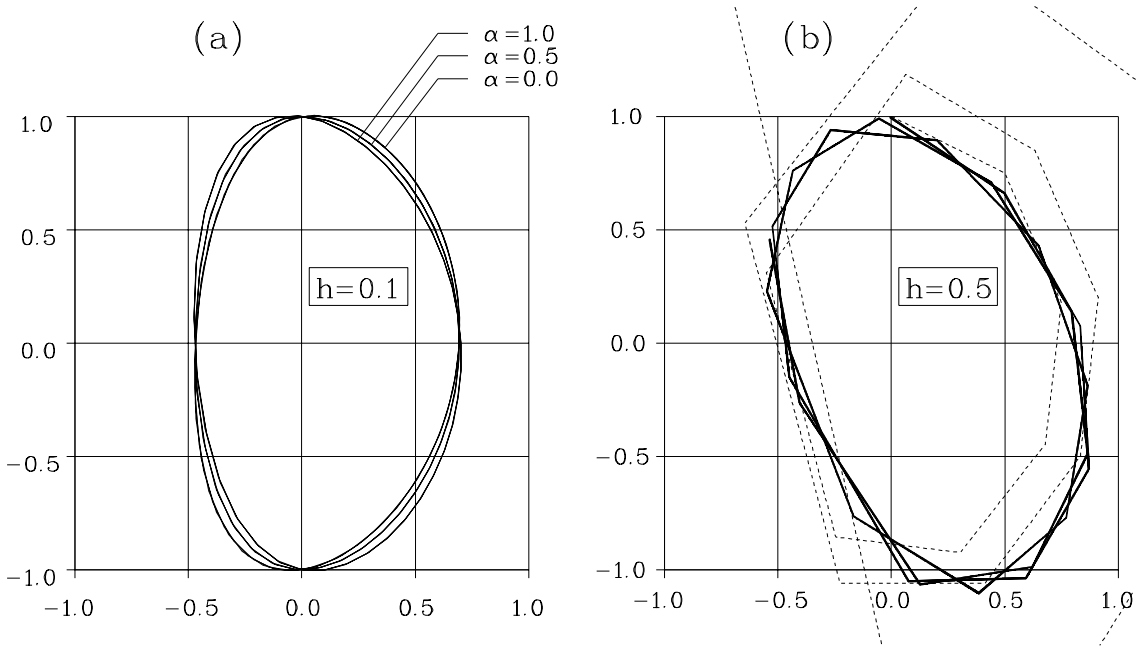

Figure 6: Motion of a bar in the phase plane.

is for h=1.0 and α=1.0. Here we have the explicit formula (no iterations) for which we need 15 time steps.

6 Numerical examples.

More complex numerical examples prove high efficiency of the presented approach to problems of evolution of geometry. Two examples of viscoplastic deformation are presented below. The first one is the benchmark. The cylinder (H=3.24 cm, R=0.32 cm, ρ=8.93 g/cm^3, K=0.005, m=0.1) hits a rigid base with a speed v=0.0227 cm/μs. The computation was performed with α=0.5 and h=1 μs in 80 steps (Fig. 8). Finally, the following results were obtained: height 2.12 cm, radius 0.71 cm, maximum strain 3.0. Other authors got the following range of values: height 2.08—2.16 cm, radius 0.67—0.72 cm, maximum strain 2.6—3.2. It is essential that other methods (for example [11, 12]) require 9500 steps or 3200—12600 cycles. On

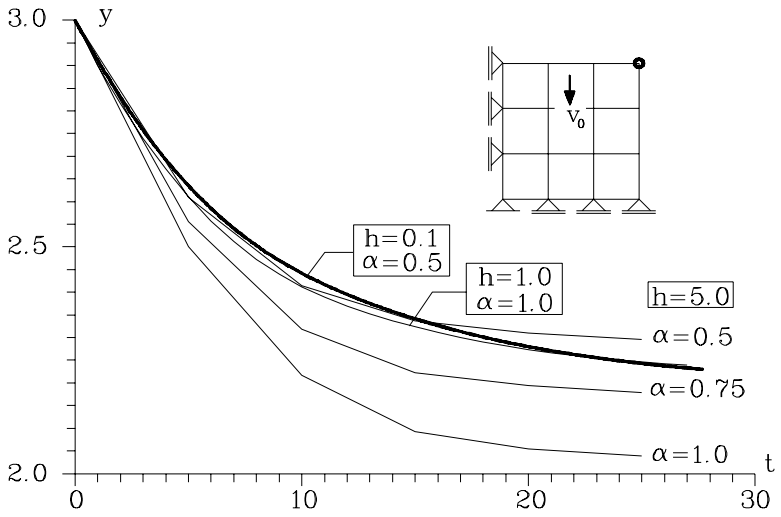

Figure 7: Test of viscoplastic deformation.

this background the space–time approach is much more efficient. The second example has 1250 spatial quadrangular elements. The axi–symmetric viscoplastic cylinder (H=10 cm, R_{int}=2 cm, R_{ext}=2.2 cm) is crashed with a speed v=180 km/h. The calculation lasts longer in this case since an internal contact is considered. There is no friction between parts of the material. The deformed mesh and 3–dimensional view is depicted in Fig. 8 and 9.

7 Conclusions

In the paper we have presented a new approach to the space–time finite element method. The formulation is based on the velocity vector as a basic parameter. Problems with nonlinear geometry evolution can simply and efficiently be solved. In this case we can choose both the explicit and implicit scheme. Real engineering problems can be solved with a small number of time steps and small number of iterations per step.

The properties of the time integration scheme depend on the parameters of the formulation. The accuracy, degree of approximation, reduction of higher mode

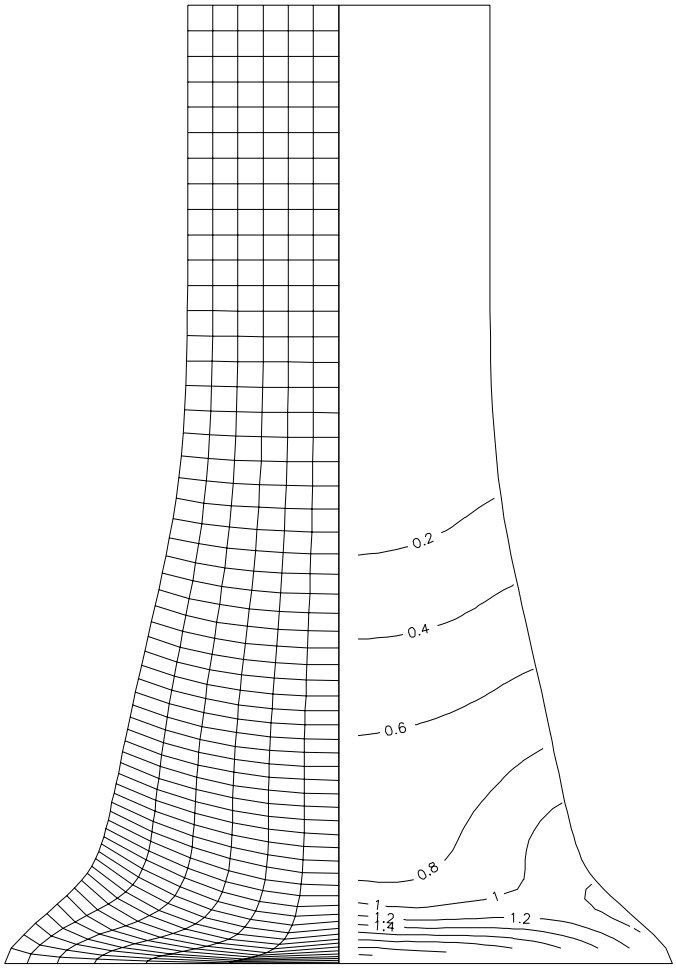

Figure 8: Impact of a bar – deformed mesh and generalized strain.

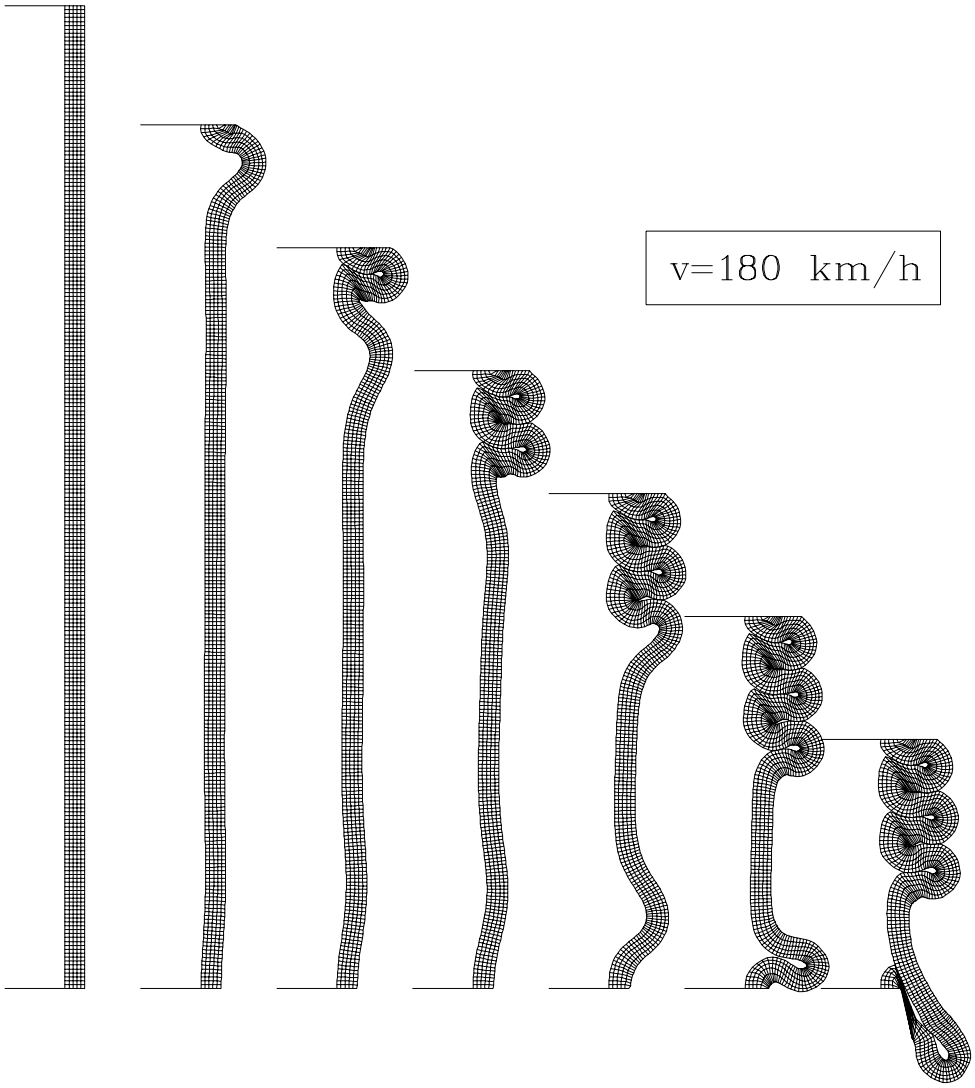

Figure 9: Finite element mesh in successive stages.

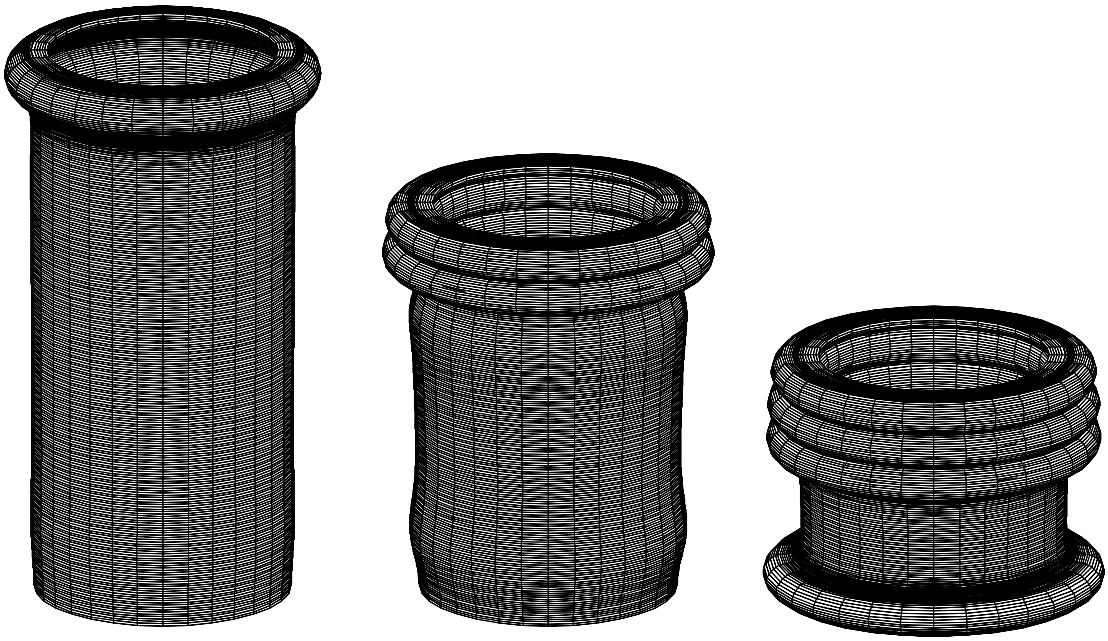

Figure 10: 3–D view of the axi–symmetric cylinder in chosen moments.

oscilations were investigated. Comparison with other numerical time integration methods can be done but direct relation between the methods is impossible. All the methods developed to date are derived for the integration with constant coefficients. The method presented in the paper is prepared for problems of evolution. One–degree-of–freedom system is only the particular case.

References

[1] J.T. Oden. A generalized theory of finite elements, II. Applications. *Int. J. Numer. Meth. Engng.*, 1:247–259, 1969.

[2] Z. Kączkowski. The method of finite space–time elements in dynamics of structures. *J. Tech. Phys.*, 16(1):69–84, 1975.

[3] Z. Kączkowski. General formulation of the stiffness matrix for the space–time finite elements. *Archiwum Inż. Ląd.*, 25(3):351–357, 1979.

[4] C.I. Bajer. Adaptive mesh in dynamic problem by the space–time approach. *Comput. and Struct.*, 33(2):319–325, 1989.

[5] C. Bajer and A. Podhorecki. Space–time element method in structural dynamics. *Arch. of Mech.*, 41:863–889, 1989.

[6] C. Bohatier. A large deformation formulation and solution with space–time finite elements. *Arch. Mech.*, 44:31–41, 1992.

[7] C. Bajer. Space–time finite element formulation for the dynamical evolutionary process. *Appl. Math. and Comp. Sci.*, 3(2):251–268, 1993.

[8] H.M. Hilber, T.J.R.Hughes, and R.L. Taylor. Improved numerical dissipation for time integration algorithms in structural dynamics. *Earthquake Engng and Struct. Dyn.*, 5:283–292, 1977.

[9] Z. Kacprzyk and T. Lewiński. Comparison of some numerical integration methods for the equations of motion of systems with a finite number of degrees of freedom. *Eng. Trans.*, 31(2):213–240, 1983.

[10] N.J. Hoff. Approximate analysis of structures in the presence of moderately large creep deformation. *Q. Appl. Math.*, 12(1):49, 1954.

[11] R.E. Dick and W.H. Harris. Fully automated rezoning of evolving geometry problems. In *Numerical methods in industrial forming processes*, pages 243–248. Balkema, 1992.

[12] J.-Ph. Ponthot. The use of the Eulerian–Lagrangian formulation including contact: Applications to forming simulation via FEM. In *Numerical methods in industrial forming processes*, pages 293–300. Balkema, 1992.